ELSEVIER

Biochimica et Biophysica Acta 1511 (2001) 297–308

BIOCHIMICA ET BIOPHYSICA ACTA

BBA

www.bba-direct.com

Thermal transitions of DMPG bilayers in aqueous solution: SAXS structural studies

Karin A. Riske, Lia Q. Amaral, M. Teresa Lamy-Freund *

Instituto de Fisica, Universidade de S. Paulo, CP 66318, CEP 05315-970, São Paulo, SP, Brazil

Received 1 December 2000; received in revised form 23 January 2001; accepted 25 January 2001

Abstract

Dimyristoylphosphatidylglycerol (DMPG) has been extensively studied as a model for biological membranes, since phosphatidylglycerol is the most abundant anionic phospholipid in prokaryotic cells. At low ionic strengths, this lipid presents a peculiar thermal behavior, with two sharp changes in the light scattering profile, at temperatures named here T_m^{on} and T_m^{off}. Structural changes involved in the DMPG thermal transitions are here investigated by small angle X-ray scattering (SAXS), and compared to the results yielded by differential scanning calorimetry (DSC) and electron spin resonance (ESR). The SAXS results show a broad peak, indicating that DMPG is organized in single bilayers, for the range of temperature studied (10–45°C). SAXS intensity shows an unusual effect, starting to decrease at T_m^{on}, and presenting a sharp increase at T_m^{off}. The bilayer electron density profiles, obtained from modeling the SAXS curves, show a gradual decrease in electron density contrast (attributed to separation between charged head groups) and in bilayer thickness between T_m^{on} and T_m^{off}. Results yielded by SAXS, DSC and ESR indicate that a chain melting process starts at T_m^{on}, but a complete fluid phase exists only for temperatures above T_m^{off}, with structural changes occurring at the bilayer level in the intermediate region.

Keywords: Dimyristoylphosphatidylglycerol; Thermal transition; Small angle X-ray scattering; Differential scanning calorimetry; Electron spin resonance

1. Introduction

Since the majority of the cell membranes have a net negative charge, the study of charged model membranes has been considered of great importance for the understanding of many biochemical processes. Phosphatidylglycerol is the most abundant anionic phospholipid present in prokaryotic cell membranes and has been extensively studied as a model for negative membranes [1–3]. Therefore, most studies with charged membranes have been carried out under physiological conditions (ionic strength around 150 mM). However, it has been shown that, under different conditions of pH, ionic strength, lipid concentration and time of incubation at low temperatures, aqueous dispersions of dimyristoylphosphatidylglycerol (DMPG) present interesting physico-chemical properties [2,4–11], which also received theoretical modeling [12,13].

In a range of low ionic strength, DMPG presents a specific thermal behavior, with the presence of two sharp changes in the light scattering thermal profile, thus defining three different regions. At low and high

* Corresponding author. Fax: +55-11-3813-4334; E-mail: mtfreund@if.usp.br

0005-2736/01/$ – see front matter
PII: S0005-2736(01)00287-5

temperatures, the sample is turbid, whereas between the transitions a transparent and viscous phase is observed [2,10,14]. The first transition has been associated with the bilayer gel to liquid crystalline main phase transition (approx. 20°C), as a simultaneous decrease in chain packing is observed with spin labels incorporated in the membrane [10]. The second transition observed by light scattering, named previously the posttransition (approx. 30°C), is characteristic of DMPG, and no sharp changes in chain mobility were detected at this temperature. For reasons that will become clear in this paper, these temperatures are now renamed as T_m^{on} and T_m^{off}, respectively (onset and offset of the melting regime).

We have proposed [10] that the great decrease in light scattering at T_m^{on} was caused by an increase in intervesicle repulsion. That would be related to an increase in the modulus of the electrostatic surface potential (Ψ_o), due to the dissociation of sodium ions from the phosphatidylglycerol (PG) head groups at the transition temperature. The increase in the electrostatic surface potential at T_m^{on} was measured in a subsequent work [11], by the partitioning of a cationic aqueous soluble spin label between the membrane negative surface and the bulk water solution. Reasonable values of Ψ_o were obtained for DMPG dispersions at different ionic strengths and compared with those yielded by the Gouy-Chapman-Stern model. The absence of vesicle fusion was established by the analysis of the electron spin resonance (ESR) spectra of phospholipid spin labels incorporated in a fraction of the DMPG vesicles: the probes do not spread out through all the DMPG bilayers present in the sample, even upon crossing the thermal transitions [11]. In contrast to that result, it was suggested that DMPG in the transparent and viscous phase (between T_m^{on} and T_m^{off}) arranges itself in a three-dimensional lipid network without the formation of vesicles, which would be present in the two neighboring phases [2,13].

Small angle X-ray scattering (SAXS) has been widely used to characterize the structure of aqueous dispersions of lipid bilayers. Many lipids are known to arrange themselves in multibilayer structure with a repeat distance of a few nanometers, thus giving rise to Bragg diffraction in the small angle region. Whereas many studies have been done on zwitterionic phospholipids [15–22], mainly with lecithin, charged membranes have not been systematically investigated, especially at low ionic strength conditions.

In the present work, the SAXS technique was used to reveal the bilayer structural changes involved in the DMPG melting transition at low ionic strength. Whereas our previous works were done with 10 mM DMPG, the present one is carried out on 50 mM DMPG to fulfill the requirement of higher intensities in SAXS measurements. Other techniques were employed to complement the SAXS structural information: turbidity measurements, differential scanning calorimetry (DSC) and electron spin resonance.

2. Materials and methods

2.1. Materials

The sodium salt of the phospholipid DMPG (1,2-dimyristoyl-*sn*-glycero-3-[phospho-*rac*-glycerol]) and DMPC (1,2-dimyristoyl-*sn*-glycero-3-[phosphocholine]) were purchased from Avanti Polar Lipids (Birmingham, AL, USA). The spin label 14-PCSL (1-palmitoyl-2-(14-doxyl stearoyl)-*sn*-glycero-3-phosphocholine) was a kind donation of Dr. A. Watts from the Oxford University (Oxford, UK). The buffer system used was 10 mM HEPES (4-(2-hydroxyethyl)-1-piperizineethanesulfonic acid) adjusted with NaOH to pH 7.4. The ionic strength was calculated and measured to be 4 mM. Mille-Q Plus water (Millipore), pH $\approx$ 6, was used throughout.

2.2. Lipid dispersion preparation

A lipid film was formed from a chloroform solution of lipids, dried under a stream of N_2 and left under reduced pressure for a minimum of 2 h, to remove all traces of the organic solvent. Vesicles were prepared by the addition of the HEPES buffer with 2 mM added NaCl, followed by vortexing for about 2 min above T_m^{off} (around 40°C). The samples were kept at room temperature and used within a few hours after preparation. For the ESR measurements 0.3 mol% 14-PCSL was added to the chloroform lipid solution. At this lipid/spin label relative concentration no spin exchange linewidth broadening occurred. The experimental results here reported, for all techniques, were obtained by increasing the tem-

perature, leaving the sample for at least 5 min at each temperature. Nevertheless, the experiments were found to be reversible, and very similar results were obtained by decreasing the temperature.

2.3. Turbidity measurements

Optical absorption measurements at a wavelength of 280 nm were carried out with a spectrophotometer HP 8452 A. The temperature was maintained with an external water bath circulator, and measured with a Fluke 51 K/J thermometer placed inside the cuvette. The optical path used was 2 mm.

2.4. Differential scanning calorimetry

The calorimetric data were carried out in a Microcalorimeter Microcal MC-2. The scan rate used was 20°C/h. The baseline subtractions and peak integrals were done using the Microcal Origin software with the additional device for DSC data analysis provided by Microcal.

2.5. ESR spectroscopy

ESR measurements were performed with a Bruker EMX spectrometer. Field-modulation amplitude of 1 G and microwave power of 5 mW were used. The temperature was controlled to about 0.2°C with a Bruker BVT-2000 variable temperature device. The temperature was always monitored with a Fluke 51 K/J thermometer with the probe placed just above the cavity. The magnetic field was measured with a Bruker ER 035 NMR Gaussmeter. Spectral parameters were measured using the Win-EPR software.

2.6. Small angle X-ray scattering

Measurements were done in the SAXS beam line of the LNLS (National Laboratory of Synchrotron Radiation, Campinas, SP, Brazil), with a one-dimensional sensitive position detector. Samples were conditioned in flat sample holders with mylar windows. The X-ray wavelength used was $\lambda = 1.6$ Å, and the sample-detector distances were 62.65 cm (higher intensity) and 91.3 cm. Data were normalized for the acquisition time (20–40 min), monitor integral counts (to compensate for oscillations in the beam intensity), and corrected for detector response and sample attenuation. The scattering due to the buffer was subtracted from all SAXS curves. The fitting to the experimental curves was done with the Microcal Origin software.

3. Results and discussion

3.1. Turbidity

Turbidity measurements performed on 50 mM DMPG at low ionic strength (10 mM HEPES pH 7.4+2 mM NaCl) show that this system presents a light scattering thermal profile similar to that yielded by the 10 mM DMPG dispersion [10], with two abrupt changes at the temperatures called now T_m^{on} and T_m^{off}. However, results for 50 mM now obtained show slightly higher T_m^{on} (19°C) and lower T_m^{off} (30°C) values than those yielded by the less concentrated 10 mM dispersion.

3.2. DSC

Fig. 1 shows the heat capacity Cp measured for DMPG at low ionic strength and for DMPC. The zwitterionic lipid DMPC presents a pretransition at 13°C and a very sharp and strong T_m peak at 23.5°C. The molar enthalpy of the DMPC main transition is $\Delta H = 5.0 \pm 0.8$ kcal/mol, as expected [23]. A similar

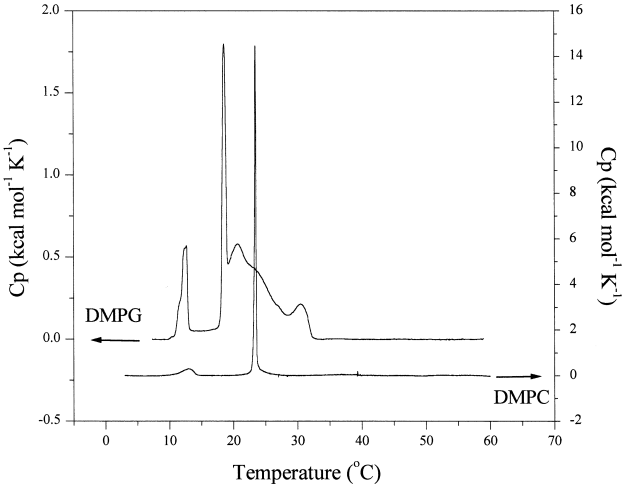

Fig. 1. Differential scanning calorimetry of 50 mM DMPG in HEPES buffer+2 mM NaCl and 1 mM DMPC in HEPES buffer. Scan rate: 20°C/h.

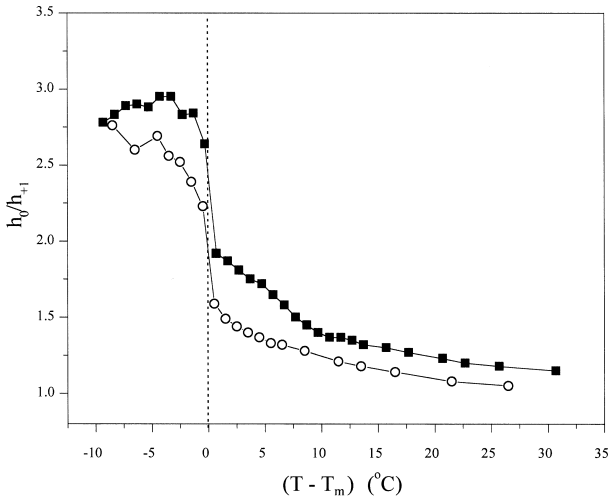

Fig. 2. Temperature dependence of the ratio between the amplitudes of the central and low field resonance lines (h_0/h_{+1}) measured on the ESR spectra of 0.3 mol% 14-PCSL incorporated in (■) 50 mM DMPG in HEPES buffer+2 mM NaCl, and in (○) 10 mM DMPC in HEPES buffer. T_m^{on} is the temperature where a sharp decrease in the ratio h_0/h_{+1} was observed.

result was obtained for DMPG at high ionic strength ($\Delta H = 5.7 \pm 0.8$ kcal/mol, results not shown), a system that does not present a low light scattering region [10]. In contrast, a complex calorimetric profile is observed for 50 mM DMPG at low ionic strength, similar to the results presented by Schneider et al. [13] for 10 mM DMPG. The transition observed at 12°C is called the pretransition (T_p), with a molar enthalpy of $\Delta H = 1.0 \pm 0.2$ kcal/mol, similar to the one yielded by DMPC ($\Delta H = 0.8 \pm 0.2$ kcal/mol, Fig. 2). In the DMPG profile, the sharpest peak at 19.6°C ($\Delta H \approx 1$ kcal/mol) coincides with the temperature of the decrease in sample light scattering, here called T_m^{on}. At $T_m^{off} = 30.5$°C, a broader and weaker transition ($\Delta H = 0.5 \pm 0.2$ kcal/mol) is observed in the DSC profile. However, DSC clearly indicates that structural changes are occurring between T_m^{on} and T_m^{off}, evidenced by the presence of a few superimposed broad Cp peaks in this region (Fig. 1).

It is noteworthy that if the complex calorimetric scan of the low ionic strength DMPG dispersion is integrated for temperatures above 15°C (including T_m^{on}, T_m^{off} and the region between them), a ΔH value rather similar to those yielded by the main transition of DMPC, or high ionic strength DMPG, is obtained, $\Delta H = 5.2 \pm 0.8$ kcal/mol. This suggests that the chain melting of the anionic DMPG bilayers at low ionic strength is spread over a large temperature range, as previously proposed by Heimburg and Biltonen [2]. Interestingly, at this low ionic strength condition, the DMPG phase transition is not a continuous process, but rather occurs in steps.

3.3. ESR

In order to obtain information on the hydrocarbon chain mobility, we have done ESR measurements with a spin label incorporated in DMPG bilayers. For comparison, experiments were also done with the well-known DMPC phospholipid. The spin label used was the 14-PCSL, a phospholipid with a choline head group well anchored at the bilayer surface and a doxyl group attached to the 14th carbon of the alkyl chain. The position of the paramagnetic center is very convenient, as spin probes deeper in the membrane core are more sensitive to changes in the bilayer viscosity [24]. Several parameters directly measured on the ESR spectra can quantify chain mobility/disorder. We have chosen the ratio of the amplitudes of the central and low field lines (h_0/h_{+1}), due to the accuracy of the measurements and its sensitivity in monitoring mobility changes. As the three absorption lines have almost equal amplitudes for very fast isotropic movements, this ratio will decrease tending to the unity as the spin label mobility increases. Fig. 2 shows the parameter h_0/h_{+1} measured on the spectra of 14-PCSL incorporated in DMPG and DMPC vesicles, as a function of ($T - T_m^{on}$). Although there is no sharp parameter variation at T_m^{off}, as previously shown [10], we clearly observe that for DMPG there is a great decrease in chain packing at T_m^{on}, followed by a smooth decrease until T_m^{off} is reached ($\Delta T \approx 10$°C). Above T_m^{off} the microviscosity of the fluid phases of DMPC and DMPG are quite similar. On the other hand, DMPC does not show this shoulder, going directly to a fluid phase after T_m. Therefore, these results are in agreement with those obtained with DSC (Fig. 1), indicating that, for DMPG, the full melting process is only finished at T_m^{off}. Though less clear, the same behavior is indicated by lipids spin labeled at the 5th and 12th carbon atom when incorporated in 10 mM DMPG (Fig. 7 in [10]), if the spectral parameters are plotted against ($T - T_m^{on}$) (not shown). It is interesting to note that the ESR spectra of 5-, 12- and 14-PCSL,

in the transition region, are not a sum of spectra of spin labels residing in domains of different fluidity. This could be an indication that the transition region corresponds to an intermediate packing, rather than a coexistence of gel and fluid patches. However, due to the loose packing of the gel phase of the C_{14} chains, the spin labels could be probing both gel and fluid regions in the ESR time scale, averaging out the two different packing regions.

3.4. SAXS

We have done SAXS measurements on 50 mM DMPG at low ionic strength (HEPES buffer+2 mM NaCl) in the temperature range between 10°C and 45°C. SAXS curves were obtained for three different preparations to check reproducibility. SAXS of 10 mM DMPG samples were also obtained, showing similar results, but with much poorer statistics, due to the lower intensities.

In the investigated q range (q being the scattering vector modulus given by $q = 4\pi \sin(\theta)/\lambda$, where 2θ is the scattering angle), from 0.012 $Å^{-1}$ to 0.5 $Å^{-1}$ (corresponding distances between 500 Å and 13 Å, $d = 2\pi/q$), the only feature observed was a defined peak around 0.12 $Å^{-1}$. Fig. 3 shows SAXS curves of 50 mM DMPG, yielded by one of the samples, at three different temperatures: 10°C (below T_m^{on}), 27°C (between T_m^{on} and T_m^{off}) and 35°C (above T_m^{off}), in the analyzed q range (for $q < 0.03$ $Å^{-1}$ there is the influence of the direct beam and for $q > 0.35$ $Å^{-1}$ a spurious peak due to kapton in the beam line is detected). Similar to the results obtained with the other techniques, both thermal transitions monitored by SAXS were reversible.

The curve shown at 10°C is below the pretransition ($T_p = 12$°C). Curves between the pre- and main transitions showed no significant differences in the peak position and intensity, in relation to the curve at 10°C, but some increase in intensity at the minimum ($q \approx 0.06$ $Å^{-1}$, $d \approx 100$ Å) could be observed in a possible 'ripple phase'. Below T_p and above T_m^{on} all curves reached zero at this minimum.

Different from many phospholipids, DMPG dispersions did not present the sharp Bragg diffraction peak characteristic of a multilamellar structure. In the well-known DMPC fluid phase a sharp Bragg peak appeared at $q = 0.095$ $Å^{-1}$ indicating a repeat

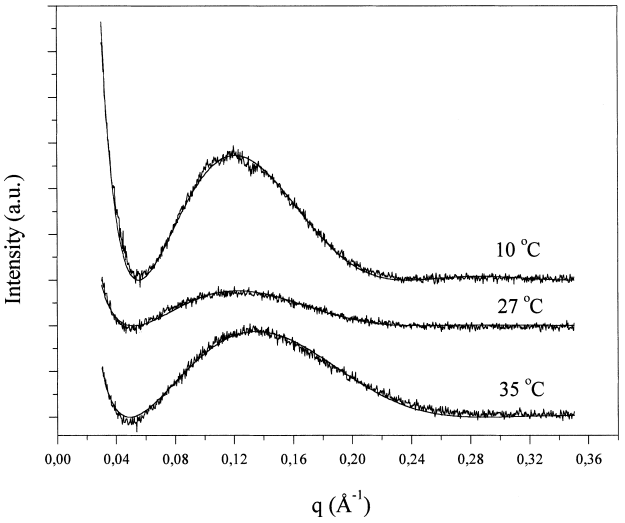

Fig. 3. SAXS curves, and corresponding theoretical fits, at three different temperatures: 10°C (below T_m^{on}), 27°C (between T_m^{on} and T_m^{off}) and 35°C (above T_m^{off}), for one of the preparations. Curves are shifted for clarity.

distance of 66 Å (result not shown), consistent with previously reported values [23]. The lamellar repeat distance corresponds to the bilayer thickness plus the water layer between the lamellae. The negatively charged phospholipid DMPG presented a broad peak at all temperatures studied.

Such a broad peak, as obtained for DMPG, is typical of a single bilayer and arises from electron density differences between the inside of the bilayer and the solvent [25]. It is possible therefore to conclude that DMPG at low ionic strength, in the measured temperature region, is organized in single bilayers, or in non-organized multilayers. A fixed amount of water (around 10–20 Å) between even two bilayers can be discarded, since it would lead to interference peaks not present in the experimental curves, as tested by us in simulations.

The temperature variation of the peak position (q_{max}) and the maximum intensity (I_{max}) for the three different preparations are shown in Fig. 4. In the gel phase the peak was centered at $q_{max} \approx 0.12$ $Å^{-1}$. Above T_m^{on}, the peak slowly shifted to higher q values, reaching $q_{max} \approx 0.13$ $Å^{-1}$ after T_m^{off}. On the other hand, on increasing the temperature, the peak intensity started to decrease at T_m^{on} and reached its minimum value just before T_m^{off}, after which the peak intensity increased abruptly. This trend was observed for three different preparations, with T_m^{off} depending

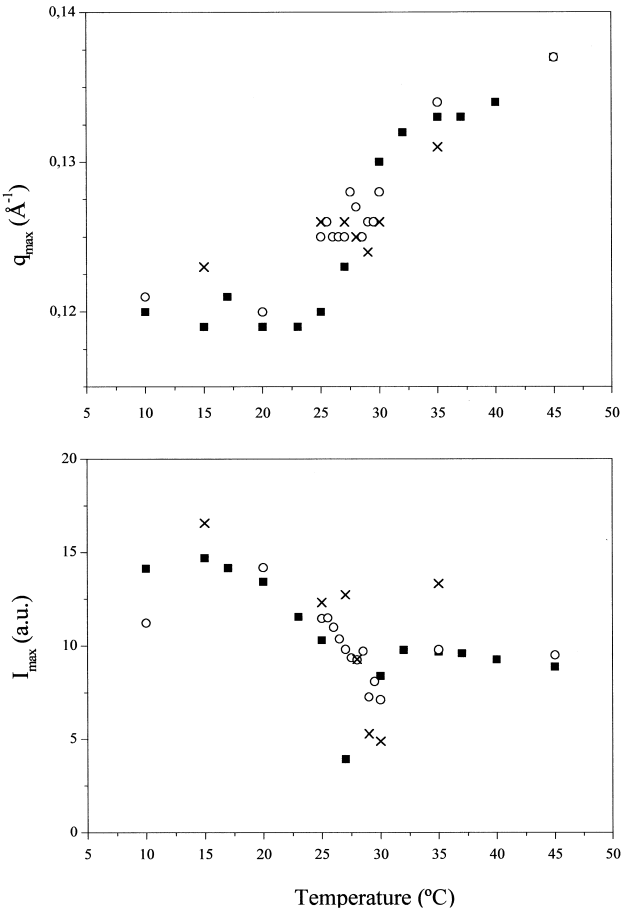

Fig. 4. Temperature dependence of the peak position (top) and maximum intensity (bottom) of the SAXS curves for three different samples (■, ○ and ×) of 50 mM DMPG in HEPES buffer+2 mM NaCl. The error in measuring the peak position was estimated to be about 1.5×10^{-3} Å^{-1} and was omitted for a better visualization of the data. The error in the intensity maximum measurement was less than the symbol size.

slightly on the sample (between 28 and 32°C), as previously discussed [11].

The shift in q_{max} (associated to a decrease in bilayer thickness) is expected at a gel-fluid transition [15]. It occurs, however, sharply at T_m for neutral phospholipids while for DMPG nothing happens at T_m^{on}, which apparently only triggers the beginning of a process that is completed only at T_m^{off}. Hence, in agreement with the DSC and ESR results, the SAXS data show that a complete fluid phase exists only for temperatures above T_m^{off}. Our results give therefore support to previous proposals relating the observed thermal changes to a 'melting regime' rather than 'melting temperatures' [2].

The decrease in the X-ray scattering intensity in the melting regime is a remarkable and unusual result. I_{max} is not sensitive to T_m^{on}, which merely corresponds to the onset of the process. T_m^{off}, on the other hand, is marked by the extremely low intensity before and a recovered intensity afterwards. A decrease in intensity of a factor 4 is observed in the intermediate region. At T_m^{off} the intensity increases by a factor of 2.7.

3.4. Analysis of the SAXS curves

Decreases in intensity could come from interference between scattering units. However, a decrease of this magnitude would imply, by necessity, the existence of an increase in intensity, associated with a large correlation peak, at lower q values. No 'ripple peak' due to correlation in the membrane surface is seen above T_m^{on} in the measured q range. Correlation between adjacent bilayers, either between opposed bilayers in the same vesicle, or between adjacent vesicles (or even between infinite bilayers in an extended network), is expected in the region 500–1600 Å for 50 mM DMPG dispersion. Such a region is too far away to produce defined zeros in the analyzed q region, particularly if one takes into account polydispersity of vesicles and short-range correlation of isotropic networks.

A change in symmetry of the scattering object could lead to a change in intensity. Recent results on the form factor of inhomogeneous particles of various shapes [26] have shown that the peak intensity decreases by a factor approx. 2.4 between a flat disk-like and a prolate ellipsoidal micelle of similar paraffin volume, but this requires aggregates of single chain amphiphiles, where a very large curvature can be attained. Phospholipid bilayers cannot bend so much.

There is, however, a simple explanation for the marked decrease in intensity: a decrease in the bilayer electron density contrast, which is responsible for the existence of the broad peak. A detailed model for the SAXS curves is shown in Appendix. The electron density profile $\rho(x)$ of the bilayer is approached by a three-level function, representing the head groups (ρ_1, R_1), the alkyl chains (ρ_2, R_2), and the methyl groups (ρ_3, R_3), and has the meaning of an 'effective profile'. The determination of such $\rho(x)$

does not imply a hypothesis of a single phase in the melting regime. For the understanding of the structural changes involved at T_m^{on} and T_m^{off}, the three SAXS curves showed in Fig. 3 were fitted with Eq. 5 from Appendix. A preliminary test showed that $n=2$ within the error (± 0.1). The fact that the analyzed q region could be fitted with Eq. 5 and $n=2$ means that the planar model is robust.

As the theoretical curves depended on eight parameters, many were the solutions that yielded a reasonable fit. To reduce physical inconsistent solutions, specific constraints were introduced. The same normalization factor c was imposed for all curves, in order to guarantee the same number of scattering units. The structural parameters of the bilayer were constrained to intervals consistent with values found in the literature [15,16,18–20,22,27]. The simplest model, with the bilayer being described by two electron density regions (the polar head group and the hydrophobic chains, with $R_3=0$) needed to be discarded. It was found necessary to include the methyl group as a different electron density region. This is in agreement with profiles obtained from structural data for membranes [18,22,28].

The constraints being applied, the parameter sets that gave reasonable fits showed only slight differences in their values, and a trend for the bilayer structural changes involved in the melting regime could be determined. In all fitting sets, for different preparations, a marked decrease in electron density contrast for the bilayer in the region between T_m^{on} and T_m^{off} occurred, both in the head group and CH_3 regions. The curve at 35°C was characterized by a clear decrease in the methylene chain thickness as compared to the one found for 10°C. In general, the fits at 27°C yielded intermediate R_2 values. The smooth shift in q_{max} between T_m^{on} and T_m^{off}, related to the decrease in the total bilayer thickness, is a direct consequence of the existence of a transition region. The decrease in I_{max}, on the other hand, is most probably related to a different packing of DMPG bilayers in the intermediate phase.

A good fitting set, where the trend described above is clear, is also shown in Fig. 3. The corresponding $\rho(x)$ functions are shown in Fig. 5 and the parameter values in Table 1. It should be remarked that the curve at 27°C, between T_m^{on} and T_m^{off}, could also be fitted with $\rho_2=\rho_w$ (ρ_w is the electron density of water) and the same c value, with slight changes in the other parameters.

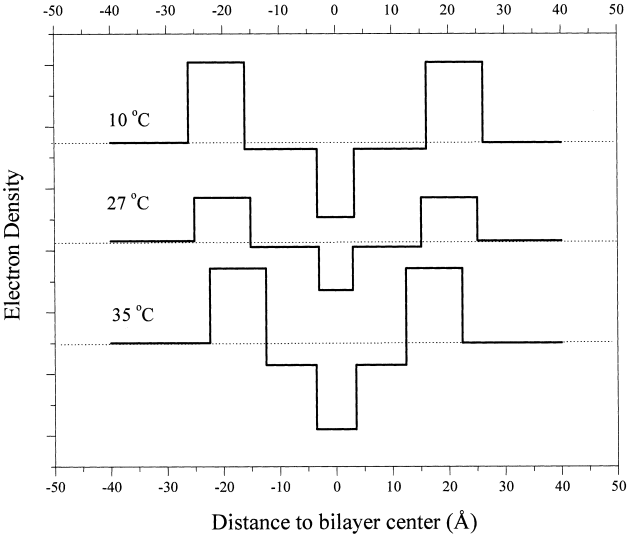

Fig. 5. Bilayer electron density profiles that yielded good fits to the SAXS curves at 10°C, 27°C and 35°C, as presented in Fig. 3. The profiles are shifted for better visualization. The dotted line represents the bulk aqueous scattering (ρ_w). The parameter values are shown in Table 1.

The fitting of curves between the pretransition and T_m^{on}, which showed non-zero intensities at the minimum, required an averaged sum of two curves with different (R_2+R_3) values, one slightly higher, the other slightly lower than the values reported for 10°C. However, a detailed analysis of such a possible ripple phase is outside the scope of the present paper, which is focused on changes between T_m^{on} and T_m^{off}.

For neutral lipids, the main phase transition has been found to basically induce a decrease in the thickness of the bilayer and a small decrease in the electron density of the alkyl chains and head groups [15]. This is consistent with the structural changes that occur as a consequence of the chains melting. We clearly see in Fig. 3 and in Table 1 that the main differences between the 10°C and 35°C bilayer density profiles are the ones expected to happen in a gel-fluid phase transition. However, the bilayer at 27°C has an intermediate chain length and rather low head group and high CH_3 electron densities. The electron density contrast in the head group region ($\Delta\rho_1$) decreases by almost a factor of 2, going from 0.13 at 10°C to 0.07 at 27°C. The decrease in electron density absolute values is, however, much smaller (see

Table 1
Parameters used in the fittings of the SAXS curves (Fig. 3): the thickness (R) and the electron density (ρ) of the head group (1), the alkyl chain (2) and the methyl group (3) bilayer regions

	R_1 (Å)	R_2 (Å)	R_3 (Å)	t (Å)	ρ_1 (e/Å^3)[a]	ρ_2 (e/Å^3)[a]	ρ_3 (e/Å^3)[a]
10°C	10.0	12.8	3.3	52.2	0.46	0.32	0.21
27°C	10.0	12.1	3.0	50.2	0.40	0.32	0.25
35°C	10.0	8.9	3.5	44.8	0.45	0.29	0.19

The total bilayer thickness, $t = R_1 + R_2 + R_3$, is also given. $c = 0.012$, $n = 2$.
[a]Absolute values were obtained considering the water electron density $\rho_w = 0.33$ e/Å^3 [18] and fixing the methylene electron density in the gel phase at $\rho_2^{gel} = 0.32$ e/Å^3 [16].

Table 1). Such a decrease could be related to a local increase in the surface area, due to separation between polar head groups. For a constant R_1, the drop of 13% in ρ_1 corresponds to an increase in head group area of the same percentage, and an increase in head group separation of 6.5% would be enough to explain the drop in intensity. An increase in the methyl group packing at 27°C is also seen, since R_3 decreases and ρ_3 increases. This could indicate a small interdigitation between the monolayers. The alkyl chain density, ρ_2, practically does not change, whereas R_2 decreases. The abrupt increase in I_{max} at T_m^{off} corresponds to a final rearrangement of the chains in a packed but fluid state, with a decrease in the mean area per head group, in view of the increase in ρ_1 observed after T_m^{off} (35°C in Fig. 5 and Table 1). It is seen therefore that the decrease in I_{max} can be explained in terms of acceptable structural changes at the bilayer level. The separation between charged head groups could also correlate with local fluctuations in membrane curvature and disruptions with water penetration.

To sum up, some defined facts emerge from the SAXS results and the obtained fitting parameters. (i) A single bilayer is the basic structure over the whole temperature interval. Changes in surface curvature do not seem to break the planar symmetry. (ii) The parameters indicate that the dominant process is the separation of the charged head groups, initiated at T_m^{on}, not accompanied by complete melting of the chains, since only a small contraction of the thickness occurs, with some interdigitation at the CH_3 position. (iii) Only when the head group separation reaches a maximum value, near T_m^{off}, complete melting is achieved and electron density contrast is partially recovered.

4. General discussion

DSC, ESR and SAXS results show that, for DMPG dispersions at low ionic strength, a complete fluid phase exists only for temperatures above T_m^{off}, in agreement with previous proposals relating the observed thermal changes to a 'melting regime' [2]. Whereas these three techniques show that structural changes occur inside the bilayer in the temperature region between T_m^{on} and T_m^{off}, turbidity measurements, that monitor larger scale events, show sharp transitions both at T_m^{on} and T_m^{off}, and no relevant changes between them. It is interesting to note that there is a correlation between the thermal profiles of SAXS and light scattering intensities, both presenting an unusual decrease in the transition region, so far not observed for any other lipid.

In lipid bilayers, the melting of the hydrocarbon chains occurs at a temperature defined by the interchain and head group interactions [23]. However, different from the neutral or zwitterionic lipids, the interactions between head groups in charged membranes are highly sensitive to variations on experimental conditions, such as ionic strength, pH and temperature. This is attested, for instance, by the strong dependence of the DMPG main transition on sample ionic strength [29] and pH [4].

In a previous study [10] it was proposed that at T_m^{on} (there called T_m) a dissociation process of the sodium ions associated with the PG head groups was triggered, thus increasing the membrane surface potential with correlated changes in viscosity and light scattering. The increase in the magnitude of the vesicle surface potential was later confirmed by the increase in the surface partition ratio of a cationic aqueous soluble spin label [11]. At the level of the

bilayer, which is the SAXS scale, the increase in the PG ionization coefficient by the release of sodium ions would correspond only to a small change in the head group electron density, since Na^+ corresponds to less than 10% of the total glycerol number of electrons. Furthermore, the dislocated sodium ions may be substituted by water, with no significant decrease in electron density. The most important effect, however, would be a strong repulsion between adjacent head groups, which would tend to separate them. This separation could certainly be responsible for the decrease in electron density at the polar region, as discussed in the previous section, and to the beginning of the melting process. Moreover, there could be the presence of both gel and fluid domains throughout the transition region. This would certainly induce membrane deformations imposed by the coexistence of rigid and flat gel patches with soft and highly curved fluid ones, as attested by optical observation of giant vesicles [30,31]. The presence of these highly curved patches could also cause a decrease in the head group density. The discontinuous recovery of intensity at T_m^{off} would represent a rearrangement of the lipid packing that would bring the membrane to a homogeneous fluid state. Although there is no indication of a decrease in the membrane electrostatic surface potential at T_m^{off}, caused by a possible ion recondensation [11], an increase and decrease in reduced conductivity is observed at T_m^{on} and T_m^{off}, respectively [10].

Considering that, in the low ionic strength DMPG samples studied here, the lipid gel to liquid crystalline transition does not happen abruptly, it seems that there is a competition among the different temperature dependent lipid-lipid interactions. The increase in the vesicle surface charge probably induces two opposite effects: the head group separation, which favors chain melting, and the intra-bilayer repulsion between monolayers, which favors larger bilayer thickness, hence chain stiffness. Therefore, the several kinks that characterize the melting of the chains would not occur all at a single T_m, but they would be spread between T_m^{on} and T_m^{off}. This effect could also bring the coexistence of domains with different packing characteristics. Yet, some cooperative structural changes (possibly some initial kink or the release of sodium ions) occur at T_m^{on}, attested by the narrow Cp peak observed in the DSC profile (Fig. 1), and the sharp ESR parameter variation (Fig. 2). Furthermore, the presence of charges in the membrane surface hinders the formation of multilamellar vesicles, as attested by the absence of a lamellar repeat distance in the SAXS curves.

The SAXS results can be explained solely in terms of changes in the bilayer packing through the gel-fluid transition, and do not require the presence of an extended lipid network in the intermediate viscous phase, as proposed by Schneider et al. [13] from electron microscopy results. A conventional isotropic lipid network (sponge phase L_3) seems not to be present in the intermediate phase, since sponge phases present transient flow birefringence and occur near a phase with long range positional order, as lamellar or cubic [32–34], both requirements being not present in DMPG. Also, the intermediate DMPG phase does not seem to correspond to any of the known lipid network structures, since in such structures the lipid bilayer is always in the liquid-crystalline state. From the SAXS results, a lipid network does not seem probable as a stable phase over the whole temperature range between T_m^{on} and T_m^{off}, as no abrupt change in the SAXS curves is observed at T_m^{on}. Furthermore, a transformation of vesicles into lipid networks would imply a process of fission and fusion of bilayers, and we have shown [11] that no relevant lipid rearrangement between vesicles occurs when crossing the thermal transitions, since no decrease in spin exchange was observed upon diluting a highly labeled DMPG dispersion into a pure DMPG sample. Further investigation at the mesoscopic scale, as well as on structure and dynamics of the counterions and amphiphile molecules, is necessary to completely elucidate the phenomenon.

The results presented here suggest a possible very interesting aspect of the behavior of DMPG, and possibly of some other charged membranes, which may have biological importance. The membrane 'melting process' seems to be triggered from the outside surface, starting due to an increase in the electrostatic repulsion between the polar head groups, instead of being triggered from the inside by intra- and interchain interactions.

Acknowledgements

We thank Dr. Iris Torriani, responsible for the SAXS line at LNLS, and Dr. H.-G. Döbereiner and Dr. G. Brezesinski, for the use of the DSC equipment. K.A.R. has a FAPESP doctorate fellowship. Financial support from USP, FAPESP and CNPq is acknowledged. Research was also partially supported by LNLS (Laboratório National de Luz Sincrotron) and PRONEX/CNPq/MCT project.

Appendix. Model for the SAXS curves

The X-ray intensity for a single flat particle (membrane in this case) averaged over all directions in space is given by [25]:

$$I_1(q) = A\frac{2\pi}{q^2}F_t^2(q) \quad (1)$$

A is the area of the flat membrane and $F_t(q)$ is the bilayer transversal form factor, given by:

$$F_t(q) = \int_{-t/2}^{+t/2} \rho(x)\cos(qx)\mathrm{d}x \quad (2)$$

$\rho(x)$ is the profile of electron density in the direction perpendicular to the bilayer plane and t is the bilayer thickness.

The q^{-2} factor in Eq. 1 is a fingerprint of planar symmetry. In the case of cylindrical symmetry, a factor q^{-1} should appear instead. So, this factor represents a good test of the symmetry.

For an assembly of N scattering membranes the intensity is

$$I(q) = NI_1(q)S(q) \quad (3)$$

$S(q)$ is the interference function, varying from 1 (no correlation) to N (perfect constructive interference) and to zero (perfect destructive interference).

In case of multilamellar vesicles in isotropic solution or birefringent smectic lamellar phases, $S(q)$ builds a sharp Bragg peak at $q = 2\pi/d$, with d the repeat distance. As already mentioned, such a pattern is not present in our results. $S(q)$ may also build a broad peak due to correlation between neighboring units. For 50 mM DMPG dispersion one expects a correlation between units (as discussed in the text) too large to be seen in the SAXS range. Therefore, in the analyzed q range it is possible to consider, in a first approximation, $S(q) = 1$ and no correlated planar bilayers as responsible for the SAXS curve.

The intensity will be thus proportional to NA, the total area corresponding to the total number of lipids forming the bilayers. Thus, within the approximation of planar and no correlated bilayers, for a given total lipid concentration, the number and size of the vesicles (too large to influence the SAXS curve) do not affect the scattered intensity. The reason for the observed changes in intensity must then be correlated to changes in the electron density contrast $\rho(x)$.

The electron density distribution $\rho(x)$ of lipid bilayers is known to be mainly divided in three different regions: the head groups, the alkyl chains and the methyl groups at the chains' end [16,27]. Thus, a simple three-step model can be used to mimic the bilayer electron density. It has been shown that, even though real bilayers do not show sharp steps in $\rho(x)$, the step model approximation yields good data interpretation [16,17].

Solving the integral (Eq. 2) in terms of the thickness and electron density parameters of the three regions, we obtain an expression for the bilayer form factor:

$$F_t(q) = \frac{2}{q}\left[2\Delta\rho_1 \sin\left(\frac{qR_1}{2}\right)\cos q\left(\frac{R_1}{2}+R_2+R_3\right)+ 2\Delta\rho_2 \sin\left(\frac{qR_2}{2}\right)\cos q\left(\frac{R_2}{2}+R_3\right)+\Delta\rho_3 \sin(qR_3)\right] \quad (4)$$

R_1, R_2 and R_3 are the thickness of the head group, alkyl chain and methyl group respectively, and $\Delta\rho_1$, $\Delta\rho_2$ and $\Delta\rho_3$ are the respective electron density contrasts of each bilayer region in relation to the bulk aqueous density ρ_w ($\Delta\rho_i = \rho_i - \rho_w$). It is important to note that the electron density and thickness of each region are not totally independent parameters. For instance, an increase in a region thickness can, sometimes, be compensated by a decrease in its electron density.

We used the following expression to fit our data:

$$I = \frac{c}{q^n}F_t^2(q) \quad (5)$$

c is a normalization constant and n is the q exponent, expected to be $n=2$ for planar symmetry.

References

[1] J. Seelig, P.M. MacDonald, P.G. Scherer, Phospholipid head groups as sensors of electric charge in membranes, Biochemistry 26 (1987) 7535–7541.

[2] T. Heimburg, R.L. Biltonen, Thermotropic behavior of dimyristoylphosphatidylglycerol and its interaction with cytochrome *c*, Biochemistry 33 (1994) 9477–9488.

[3] M.H. Biaggi, K.A. Riske, M.T. Lamy-Freund, Melanotropic peptides-lipid bilayer interaction. Comparison of the hormone α-MSH to a biologically more potent analog, Biophys. Chem. 67 (1997) 139–149.

[4] A. Watts, K. Harlos, W. Maschke, D. Marsh, Control of the structure and fluidity of phosphatidylglycerol bilayers by pH titration, Biochim. Biophys. Acta 510 (1978) 63–74.

[5] R.M. Epand, S.W. Hui, Effect of electrostatic repulsion on the morphology and thermotropic transitions of anionic phospholipids, FEBS Lett. 209 (1986) 257–260.

[6] N.L. Gershfeld, W.F. Stevens Jr., R.J. Nossal, Equilibrium studies of phospholipids bilayer assembly, Faraday Discuss. Chem. Soc. 81 (1986) 19–28.

[7] R.M. Epand, B. Gabel, R.F. Epand, A. Sem, S.W. Hui, Formation of a new stable phase of phosphatidylglycerol, Biophys. J. 63 (1992) 327–332.

[8] M. Kodama, T. Miyata, T. Yokoyama, Crystalline cylindrical structures of Na^+-bound dimyristoylphosphatidylglycerol as revealed by microcalorimetry and electron microscopy, Biochim. Biophys. Acta 1168 (1993) 243–248.

[9] Y.P. Zhang, R.N.A.H. Lewis, R.N. McElhaney, Calorimetric and spectroscopic studies of the thermotropic phase behaviour of the *n*-saturated 1,2-diacylphosphatidylglycerols, Biophys. J. 72 (1997) 779–793.

[10] K.A. Riske, M.J. Politi, W.F. Reed, M.T. Lamy-Freund, Temperature and ionic strength dependent light scattering of DMPG dispersions, Chem. Phys. Lipids 89 (1997) 31–44.

[11] K.A. Riske, O.R. Nascimento, M. Peric, B. Bales, M.T. Lamy-Freund, Probing DMPG vesicle surface with a cationic aqueous soluble spin label, Biochim. Biophys. Acta 1418 (1999) 133–146.

[12] C. Goldman, K.A. Riske, M.T. Lamy-Freund, Role of soft and hard aggregates in the thermodynamics of lipid dispersions, Physiol. Rev. E 60 (1999) 7349–7353.

[13] M. Schneider, D. Marsh, W. Jahn, B. Kloesgen, T. Heimburg, Network formation of lipid membranes: triggering structural transitions by chain melting, Proc. Natl. Acad. Sci. USA 96 (1999) 14312–14317.

[14] I.S. Salonen, K.K. Eklund, J.A. Virtanen, P.K.J. Kinnunen, Comparison of the effects of NaCl on the thermotropic behaviour of *sn*-1′ and *sn*-3′ stereoisomers of 1,2-dimyristoyl-*sn*-glycero-3-phosphatidylglycerol, Biochim. Biophys. Acta 982 (1989) 205–215.

[15] T.J. McIntosh, S.A. Simon, Area per molecule and distribution of water in fully hydrated dilaurylphosphatidylethanolamine bilayers, Biochemistry 25 (1986) 4948–4952.

[16] M.C. Wiener, R.M. Suter, J.F. Nagle, Structure of the fully hydrated gel phase of dipalmitoylphosphatidylcholine, Biophys. J. 55 (1989) 315–325.

[17] M.C. Wiener, G.I. King, S.H. White, Structure of a fluid dioleoylphosphatidylcholine bilayer determined by joint refinement of x-ray and neutron diffraction data. I. Scaling of neutron data and the distribution of double bonds and water, Biophys. J. 60 (1991) 568–576.

[18] J.F. Nagle, R. Zhang, S. Tristram-Nagle, W. Sun, H.I. Petrache, X-Ray structure determination of fully hydrated Lα phase dipalmitoylphosphatidylcholine bilayers, Biophys. J. 70 (1996) 1419–1431.

[19] W.-J. Sun, S. Tristram-Nagle, R.M. Suter, J.F. Nagle, Structure of gel phase saturated lecithin bilayers: temperature and chain length dependence, Biophys. J. 71 (1996) 885–891.

[20] M. Kodama, H. Aoji, H. Takahashi, I. Hatta, Interlamellar waters in dimyristoylphosphatidylethanolamine-water system as studied by calorimetric and X-ray diffraction, Biochim. Biophys. Acta 1329 (1997) 61–73.

[21] S. Tristram-Nagle, H.I. Petrache, J.F. Nagle, Structure and interactions of fully hydrated dioleoylphosphatidylcholine bilayers, Biophys. J. 75 (1998) 917–925.

[22] H.I. Petrache, S. Tristram-Nagle, J.F. Nagle, Fluid phase structure of EPC and DMPC bilayers, Chem. Phys. Lipids 95 (1998) 83–94.

[23] D. Marsh, in: CRC Handbook of Lipid Bilayers, CRC Press, Boca Raton, FL, 1990.

[24] R.F. Turchiello, L. Juliano, A.S. Ito, M.T. Lamy-Freund, How bradykinin alters the lipid membrane structure: a spin label comparative study with bradykinin fragments and other cations, Biopolymers 54 (2000) 211–221.

[25] O. Glatter, O. Kratky, in: Small Angle X-Ray Scattering, Academic Press, New York, 1982.

[26] F. Spinozzi, F. Carsughi, P. Mariani, C. Teixeira, L.Q. Amaral, SAS from inhomogeneous particles with more than one domain of scattering density and arbitrary shape, J. Appl. Crystallogr. 33 (2000) 556–559.

[27] P.J. Quinn, H. Takahashi, I. Hatta, Characterization of complexes formed in fully hydrated dispersions of dipalmitoyl derivatives of phosphatidylcholine and diacylglycerol, Biophys. J. 68 (1995) 1374–1382.

[28] M.C. Wiener, S.H. White, Structure of a fluid dioleoyl phosphatidylcholine bilayer determined by joint refinement of X-ray and neutron diffraction data. III. Complete structure, Biophys. J. 61 (1992) 434–447.

[29] G. Cevc, A. Watts, D. Marsh, Non-electrostatic contribution to the titration of the ordered-fluid phase transition of phosphatidylglycerol bilayers, FEBS Lett. 120 (1980) 267–270.

[30] L.A. Bagatolli, E. Gratton, Two-phase fluorescence microscopy observation of shape changes at the phase transition in phospholipid giant unilamellar vesicles, Biophys. J. 77 (1999) 2090–2101.

[31] E. Sackmann, Physical basis of self-organization and func-

tion of membranes: physics of vesicles, in: R. Lipowsky, E. Sackmann (Eds.), Structure and Dynamics of Membranes. From Cells to Vesicles, Elsevier/North-Holland, Amsterdam, 1995, pp. 213–304.

[32] G. Porte, J. Marignan, P. Bassereau, R. May, Shape transformation of the aggregates in dilute surfactant solutions: a small-angle neutron scattering study, J. Phys. Fr. 49 (1988) 511–519.

[33] R. Strey, R. Schomacker, D. Roux, F. Nallet, U. Olsson, Dilute lamellar (L_3) phases in the binary water-$C_{12}E_5$ system, J. Chem. Soc. Faraday Trans. 86 (1990) 2253–2261.

[34] D. Roux, C. Coulon, M.E. Cates, Sponge phases in surfactant solutions, J. Phys. Chem. 96 (1992) 4174–4187.